Theoret. Chim. Acta (Berl.) 59, 423–435 (1981)

THEORETICA CHIMICA ACTA

© Springer-Verlag 1981

Diatomic Interactions in Momentum Space. The $1s\sigma_g$ and $2p\sigma_u$ States of H_2^+ System

Toshikatsu Koga and Mutsuo Morita

Departments of Industrial Chemistry and of Applied Science for Energy, Muroran Institute of Technology, Muroran, Hokkaido, 050 Japan

The method of momentum electron density for interatomic interactions has been applied to the two lowest σ states of the H_2^+ system. For attractive ($1s\sigma_g$) and repulsive ($2p\sigma_u$) interactions, the behaviour of momentum density and its effect on the stabilization energy of the system are examined quantitatively. The concept of contraction and expansion of the momentum density is shown to form an important guiding principle in this approach. The origin of covalent bonding is discussed based on the energy partitioning proposed previously.

Key words: Momentum electron density – H_2^+ System.

1. Introduction

In order to obtain new insight in the nuclear rearrangement problem, recently we have developed a momentum electron density approach which permits to clarify the origin of nuclear displacements such as molecular geometries and chemical reactions in terms of a concept in momentum space instead of the traditional one in coordinate space [1]. Applying the virial theorem to a uniform scaling process [2, 3], we have derived three sets of basic equations for the energy of a system and its gradient using the momentum electron density $\rho(\boldsymbol{p})$ as a basic physical quantity [1]. Based on the first set of equations, the general behaviour of the momentum density distribution and its effect on the stabilization energy and the interatomic force have been discussed during the course of attractive and repulsive interactions starting from the separated atoms. It has been suggested that the contraction and expansion of $\rho(\boldsymbol{p})$ is an important concept which governs properties of interactions in momentum space. The results have been used to study the role of kinetic energy in chemical bonding. Possible energy partitioning

0040-5744/81/0059/0423/$02.60

in this approach has also been mentioned, which may be useful in analyzing the interaction processes.

The present study is the first quantitative application of the proposed method. For the simple but actual system of H_2^+, the predicted reorganization of the momentum density is indeed found to occur in the interaction processes. Stabilization and destabilization (or attraction and repulsion) of the system are also explained from the momentum-space viewpoint. Partitionings of the stabilization energy into atom-bond components and into parallel-perpendicular components are carried out, and their relative importance is discussed. In the next section, the basic equations and the fundamental concept in this approach are briefly summarized. The radial momentum density $I(p)$ is newly introduced which permits not only to reduce the required density information from the three-dimensional $\rho(\boldsymbol{p})$ to the one-dimensional $I(p)$, but also to connect the present method with the experimental Compton profile $J(q)$. Computational details for the present system are given in Sect. 3 and the results are discussed in Sect. 4 for the attractive $1s\sigma_g$ and repulsive $2p\sigma_u$ states.

2. Basic Equations and Fundamental Concept

In the present approach of momentum density, the kinetic energy $\Delta T(R)$ $[\equiv T(R)-T(\infty)]$, stabilization energy $\Delta E[\equiv E(R)-E(\infty)]$, and force $F[\equiv -dE(R)/dR]$ of a diatomic system with internuclear distance R are given by [1]

$$\Delta T(R)=\int (p^2/2)\Delta\rho(\boldsymbol{p};R)\,d\boldsymbol{p}, \tag{1a}$$

$$\Delta E(R)=\int (p^2/2)\Delta\bar{\rho}(\boldsymbol{p};R)\,d\boldsymbol{p}, \tag{1b}$$

$$F(R)=(1/R)\int (p^2/2)\Delta\tilde{\rho}(\boldsymbol{p};R)\,d\boldsymbol{p}, \tag{1c}$$

where $\boldsymbol{p}$ stands for momentum vector of an electron and $p=|\boldsymbol{p}|$. The difference in momentum density is taken to be

$$\Delta\rho(\boldsymbol{p};R)=\rho(\boldsymbol{p};R)-\rho(\boldsymbol{p};\infty), \tag{2a}$$

and the modified density differences $\Delta\bar{\rho}$ and $\Delta\tilde{\rho}$ are defined as

$$\Delta\bar{\rho}(\boldsymbol{p};R)\equiv(1/R)\int_R^\infty \Delta\rho(\boldsymbol{p};R')\,dR', \tag{2b}$$

$$\Delta\tilde{\rho}(\boldsymbol{p};R)\equiv\Delta\bar{\rho}(\boldsymbol{p};R)+\Delta\rho(\boldsymbol{p};R). \tag{2c}$$

Eq. (1) is our basic equation which rigorously relates the energy and force with the momentum density, and from which the guiding principle of contraction and expansion is deduced for the density behaviour. The term contraction implies a reorganization of momentum density which results in a density increase at lower

momentum with a simultaneous decrease at higher momentum, while the expansion implies the opposite reorganization. The present equations have the merit that there is no need to consider nuclear repulsions separately. This point is different from the electrostatic Hellmann–Feynman theorem in the coordinate space.

Some of the guiding principles deduced from Eq. (1) are as follows [1]:
(1) For $\Delta T<0$, $\Delta\rho$ must contract, while for $\Delta T>0$, $\Delta\rho$ must expand. The contraction of $\Delta\rho$ (and then negative ΔT) is important for the initiation and acceleration of chemical reactions (bond formations), whereas the expansion (and then positive ΔT) is important for the termination of reactions.
(2) For $\Delta E<0$ (stabilization), $\Delta\tilde{\rho}$ must contract, while for $\Delta E>0$ (destabilization), $\Delta\tilde{\rho}$ must expand. At stable equilibrium, the contraction should be maximum.
(3) For $F<0$ (attraction), $\Delta\tilde{\rho}$ must contract, while for $F>0$ (repulsion), $\Delta\tilde{\rho}$ must expand. The critical point of the contraction and expansion of $\Delta\tilde{\rho}$ corresponds to the point of $F=0$, i.e. equilibrium.
(4) For large R, behaviours of $\Delta\rho$, $\Delta\bar{\rho}$, and $\Delta\tilde{\rho}$ are parallel, while at $R=R_e$ (equilibrium distance) $\Delta\rho$ and $\Delta\bar{\rho}$ show opposite reorganizations.

Since the kinetic operator $(p^2/2)$ is angular-independent, it is possible to reduce the required density information from the three-dimensional $\rho(\boldsymbol{p})$ to the one-dimensional $I(p)$ without loss of generality and rigorousness of the approach. Using the radial momentum electron density $I(p;R)$ $[\equiv\int\rho(\boldsymbol{p};R)p^2\sin\theta_p\,d\theta_p\,d\phi_p]$, we can rewrite Eq. (1) as

$$\Delta T(R)=\int(p^2/2)\Delta I(p;R)\,dp, \tag{3a}$$

$$\Delta E(R)=\int(p^2/2)\Delta\bar{I}(p;R)\,dp, \tag{3b}$$

$$F(R)=(1/R)\int(p^2/2)\Delta\tilde{I}(p;R)\,dp, \tag{3c}$$

where

$$\Delta I(p;R)\equiv\int\Delta\rho(\boldsymbol{p};R)p^2\sin\theta_p\,d\theta_p\,d\phi_p=I(p;R)-I(p;\infty), \tag{4a}$$

$$\Delta\bar{I}(p;R)\equiv\int\Delta\bar{\rho}(\boldsymbol{p};R)p^2\sin\theta_p\,d\theta_p\,d\phi_p=(1/R)\int_R^\infty\Delta I(p;R')\,dR', \tag{4b}$$

$$\Delta\tilde{I}(p;R)\equiv\int\Delta\tilde{\rho}(\boldsymbol{p};R)p^2\sin\theta_p\,d\theta_p\,d\phi_p=\Delta\bar{I}(p;R)+\Delta I(p;R). \tag{4c}$$

$I(p)$ has the merit that it is directly connected with the experimental Compton profile $J(q)$ through the relations $J(q)=(1/2)\int_{|q|}^\infty p^{-1}I(p)\,dp$ and $I(p)=2p[dJ(q)/dq]_{q=p}$ [4]. We therefore proceed with our study using the simple and convenient density function $I(p)$ along with Eq. (3).

As noted before [1], several partitionings of the stabilization energy are possible from Eq. (3) or (1). Two partitionings are examined here which seem useful for the analyses of interactions. One is atom-bond partitioning based on the decomposition of momentum density into the one-center atomic part and the two-center bond (or interatomic) part, $I(p)=I_{\text{atom}}(p)+I_{\text{bond}}(p)$.

$$\Delta E(R)=\Delta E_{\text{atom}}(R)+\Delta E_{\text{bond}}(R), \tag{5a}$$

$$\begin{cases}\Delta E_{\text{atom}}(R)=\int (p^2/2)\Delta \bar{I}_{\text{atom}}(p;R)\,dp, & \text{(5b)}\\ \Delta E_{\text{bond}}(R)=\int (p^2/2)\Delta \bar{I}_{\text{bond}}(p;R)\,dp. & \text{(5c)}\end{cases}$$

The other is directional partitioning which results from the decomposition of the kinetic operator into parallel and perpendicular parts, $(p^2/2)=(p_\parallel^2/2)+(p_\perp^2/2)+(p_{\perp'}^2/2)$. That is

$$\Delta E(R)=\Delta E_\parallel(R)+2\Delta E_\perp(R), \tag{6a}$$

$$\begin{cases}\Delta E_\parallel(R)=\int (p_\parallel^2/2)\Delta \bar{I}_\parallel(p_\parallel;R)\,dp_\parallel, & \text{(6b)}\\ \Delta E_\perp(R)=\int (p_\perp^2/2)\Delta \bar{I}_\perp(p_\perp;R)\,dp_\perp, & \text{(6c)}\end{cases}$$

where $\Delta \bar{I}_\parallel(p_\parallel;R)\equiv\iint \Delta\bar{\rho}(\boldsymbol{p};R)\,dp_\perp\,dp_{\perp'}$ etc. The kinetic energy ΔT and the interatomic force F can be partitioned similarly.

The basic equations summarized above hold for both the exact and approximate momentum densities insofar as their parent wave functions satisfy the virial theorem. Validity of the virial theorem is a necessary condition of this method.

3. Computational Details

Although the exact wave function for the H_2^+ system is known in coordinate space [5], its Dirac–Fourier transform into momentum space is difficult [6]. Approximate but very accurate wave functions of Guillemin and Zener [7] and of James [8] are given in the form of infinite series in momentum space [9]. Therefore, we here adopted the Finkelstein–Horowitz wave function [10], which was shown to give the correct behaviour of the total, kinetic, and potential energy curves over the range of R values of interest [11, 12].

The Finkelstein–Horowitz wave function is given by [10]

$$\Psi(\boldsymbol{r})=(2\pm 2S)^{-1/2}\{1s_A(\boldsymbol{r})\pm 1s_B(\boldsymbol{r})\}, \tag{7a}$$

$$1s_A(\boldsymbol{r})=(\zeta^3/\pi)^{1/2}\exp(-\zeta|\boldsymbol{r}-\boldsymbol{R}_A|), \tag{7b}$$

where S is the overlap integral and $\boldsymbol{R}_A$ the position of nucleus A ($R=|\boldsymbol{R}_A-\boldsymbol{R}_B|$). In Eq. (7a) and hereafter, addition and subtraction represent the $1s\sigma_g$ and $2p\sigma_u$

states, respectively. The exponent $\zeta = \zeta(R)$ is optimized at every R and this guarantees the validity of the virial theorem [13] and hence the basic equations of the present approach. The Dirac–Fourier transform of Eq. (7) gives the corresponding momentum wave function [14]

$$\Psi(\boldsymbol{p}) = (2 \pm 2S)^{-1/2}\{1s_A(\boldsymbol{p}) \pm 1s_B(\boldsymbol{p})\}, \tag{8a}$$

$$1s_A(\boldsymbol{p}) = \exp(-i\boldsymbol{p} \cdot \boldsymbol{R}_A)1s(\boldsymbol{p}), \tag{8b}$$

$$1s(\boldsymbol{p}) = 2^{3/2}\zeta^{5/2}\pi^{-1}(p^2 + \zeta^2)^{-2}. \tag{8c}$$

The nuclear position (more precisely, the center of AO) enters as a phase factor in the momentum representation. The momentum electron density is then obtained by $\rho(\boldsymbol{p}) = \Psi(\boldsymbol{p})^*\Psi(\boldsymbol{p})$. Typical profiles of $\rho(\boldsymbol{p})$ are shown in Fig. 1 using contour and perspective plots. We here note that the ground-state momentum density of this system, $\rho(\boldsymbol{p}) = [2^3\pi^{-2}\zeta^5(1+S)^{-1}](p^2+\zeta^2)^{-4}(1+\cos p_z R)$, is

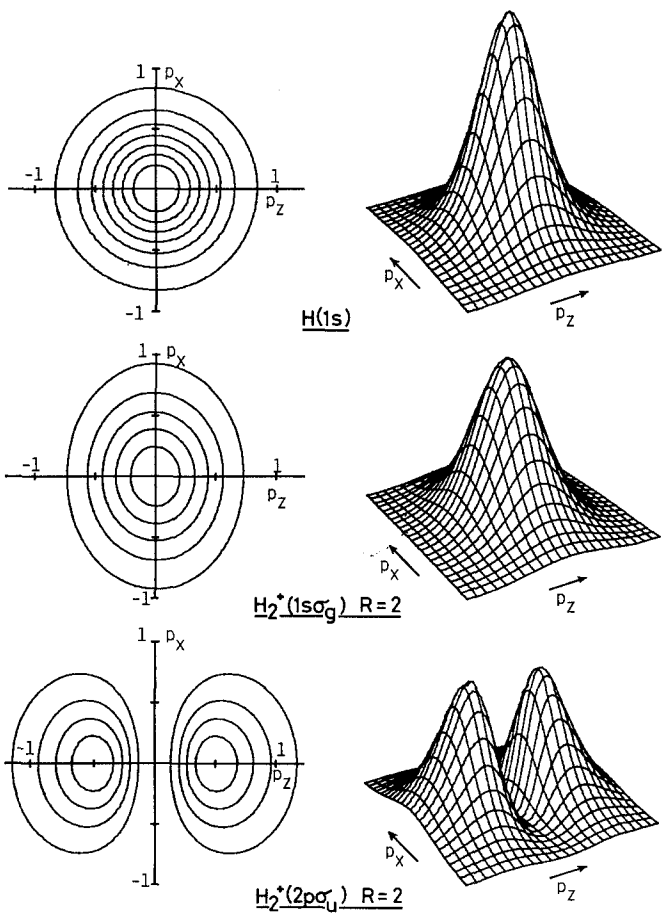

Fig. 1. Typical profiles of momentum density distribution. Contour values are 0.1, 0.2, 0.3, 0.4, 0.5, 0.6, and 0.7 a.u. from the outermost line. Perspective plots are drawn in the same scale from the same visual point. All values in atomic units

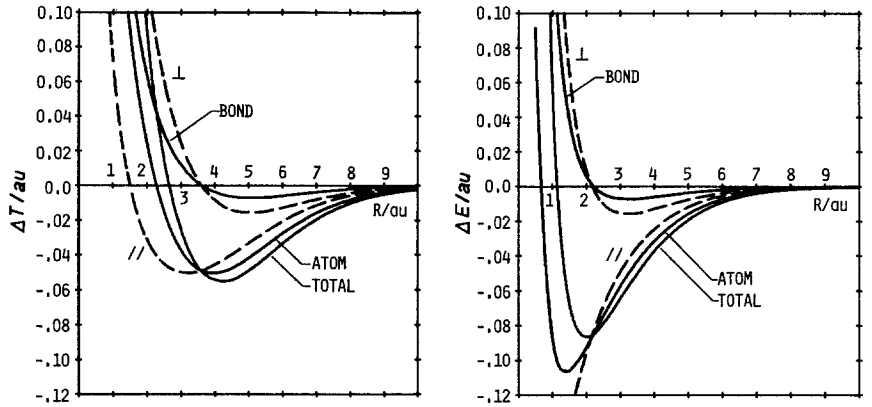

Fig. 2. $1s\sigma_g$ state. Kinetic and stabilization energies obtained from the momentum density. Their decompositions into the atm–bond and the parallel-perpendicular components are also shown

similar in form to that of a particle in a one-dimensional box with length R, $\rho(p_z) = 2\pi R^{-2}(p_z^2 - \pi^2 R^{-2})^{-2}(1 + \cos p_z R)$. This similarity may partly support the box model of diatomic momecules [15–17].

The reorganization of the momentum density from the isolated atoms is

$$\Delta\rho(\boldsymbol{p}) = \Delta\rho_{\text{atom}}(\boldsymbol{p}) + \Delta\rho_{\text{bond}}(\boldsymbol{p}), \tag{9a}$$

$$\begin{cases} \Delta\rho_{\text{atom}}(\boldsymbol{p}) = (2^3\pi^{-2})\{[\zeta^5(1 \pm S)^{-1}](p^2 + \zeta^2)^{-4} - (p^2 + 1)^{-4}\}, & (9b) \\ \Delta\rho_{\text{bond}}(\boldsymbol{p}) = \pm[2^3\pi^{-2}\zeta^5(1 \pm S)^{-1}](p^2 + \zeta^2)^{-4} \cos(pR \cos\theta_p), & (9c) \end{cases}$$

where spherical coordinates are used for $\boldsymbol{p}$ with the p_z-axis parallel to the molecular axis. The atomic part $\Delta\rho_{\text{atom}}$ is one-center part of $\rho(\boldsymbol{p})$ subtracted by the hydrogen-atomic density $\rho_{\text{H}}(\boldsymbol{p}) = 2^3\pi^{-2}(p^2 + 1)^{-4}$, while the bond part $\Delta\rho_{\text{bond}}$ is two-center part of $\rho(\boldsymbol{p})$. We see that by definition of the Finkelstein–Horowitz wave function, the atomic part (9b) is spherical, whereas the bond part (9c) induces deformation of this symmetry. The radial density difference is then given by

$$\Delta I(p) = \Delta I_{\text{atom}}(p) + \Delta I_{\text{bond}}(p), \tag{10a}$$

$$\begin{cases} \Delta I_{\text{atom}}(p) = (2^5\pi^{-1})p^2\{[\zeta^5(1 \pm S)^{-1}](p^2 + \zeta^2)^{-4} - (p^2 + 1)^{-4}\}, & (10b) \\ \Delta I_{\text{bond}}(p) = \pm[2^5\pi^{-1}\zeta^5(1 \pm S)^{-1}]p^2(p^2 + \zeta^2)^{-4}[(pR)^{-1} \sin(pR)], & (10c) \end{cases}$$

and the directional density differences are given by

$$\Delta I_{\parallel}(p_{\parallel}) = (2^3 3^{-1}\pi^{-1})\{[\zeta^5(1 \pm S)^{-1}][1 \pm cos\ (p_{\parallel}R)](p_{\parallel}^2 + \zeta^2)^{-3} - (p_{\parallel}^2 + 1)^{-3}\}, \tag{11a}$$

$$\Delta I_{\perp}(p_{\perp}) = (2^3 3^{-1}\pi^{-1})\{[\zeta^5(1 \pm S)^{-1}](p_{\perp}^2 + \zeta^2)^{-3} - (p_{\perp}^2 + 1)^{-3}\} \pm [3^{-1}\pi^{-1}\zeta^5 R^3(1 \pm S)^{-1}](p_{\perp}^2 + \zeta^2)^{-3/2}K_3(R[p_{\perp}^2 + \zeta^2]^{1/2}), \tag{11b}$$

$$\Delta I_{\perp'}(p_{\perp'}) = \Delta I_{\perp}(p_{\perp'}),$$

where $K_\nu(z)$ means the modified Bessel function [18].

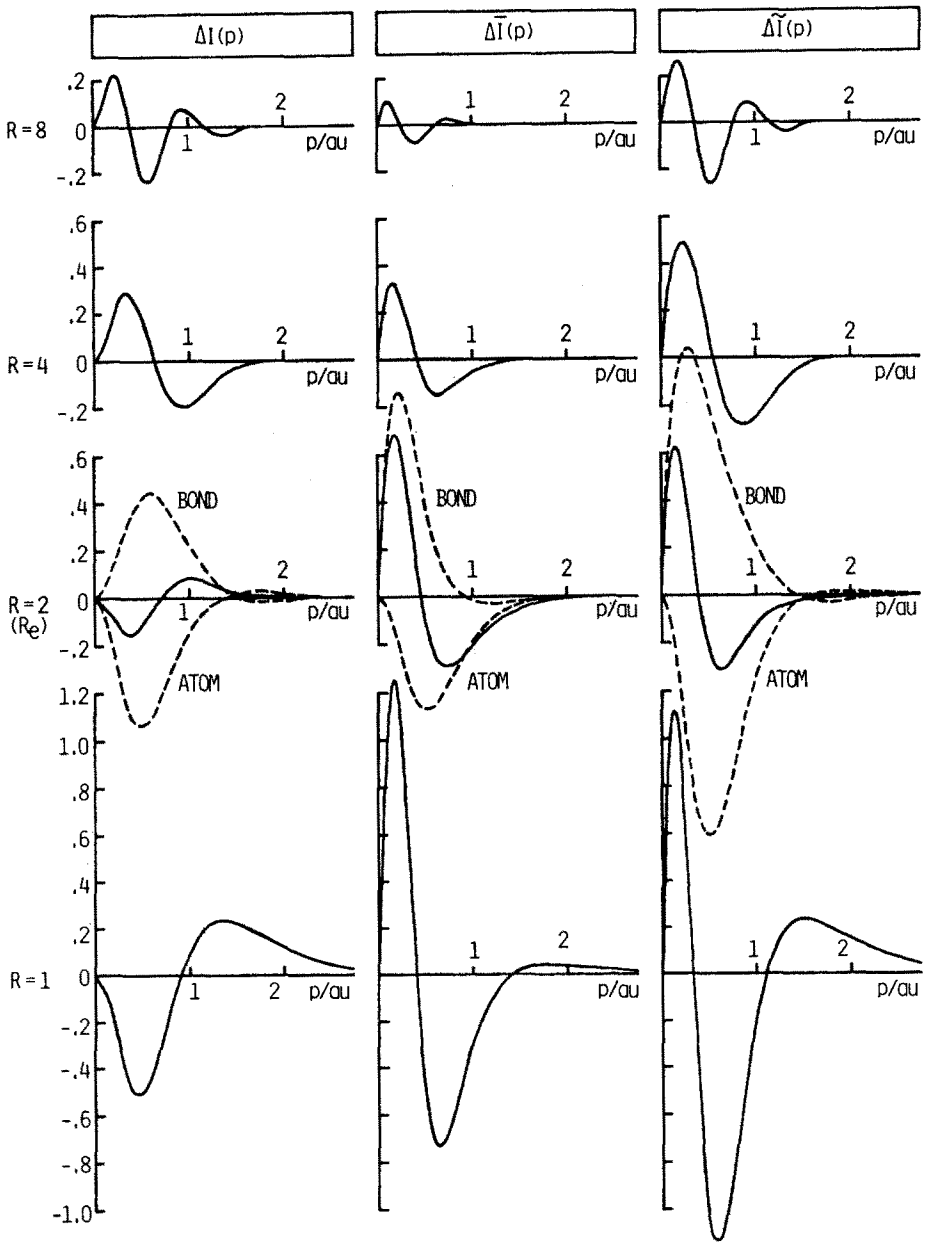

Fig. 3. $1s\sigma_g$ state. Differences in the radial momentum density distributions. The ΔI, $\Delta \bar{I}$, and $\Delta \tilde{I}$ govern ΔT, ΔE, and F, respectively. All values in atomic units

The modified density differences $\Delta\bar{I}$ and $\Delta\tilde{I}$ have been calculated numerically using the Newton–Cotes and Filon's integration formulas [18]. Evaluation of ΔE and F has been carried out similarly. However, the result for the force curve is not shown in the following analyses, since it is merely the gradient of the corresponding ΔE curve.

4. Results and Discussion

4.1. $1s\sigma_g$ State

In Fig. 2, the curves for ΔT, ΔE, and their components obtained from the momentum density are given. The total curves coincide with the results of the direct calculation. (The ΔE curve gives $R_e = 2.00$ a.u. and $D_e = 0.085$ a.u..) Their density origins ΔI and $\Delta\bar{I}$ are shown in Fig. 3 together with $\Delta\tilde{I}$ which corresponds to the force F.

In Fig. 3, the ΔI plots show contraction for $R \geq 4$ a.u., and expansion for $R \leq 2$ a.u. (The expansion is also observed in Fig. 1.) These reorganizations respectively correspond to the decrease and increase in ΔT (Fig. 2). In accord with the guiding rule, the attractive nature of the $1s\sigma_g$ state is reflected in this ΔI behaviour of initial contraction and final expansion. The critical point of the contraction/expansion of ΔI is calculated to be $R_c \simeq 2.7$ a.u. where ΔT vanishes.

The density difference $\Delta\bar{I}$ in Fig. 3 shows contraction of the momentum density for $R \geq 2$ a.u.. This is consistent with the fact that ΔE is negative (more stable than the isolated atoms) in this R-range (Fig. 2). We see that the degree of contraction increases as R lowers, corresponding to the decrease in ΔE. As shown in the $\Delta\bar{I}$ plot for $R = 2$ a.u., this contraction is a result of migration of atomic density with higher momentum into bond density with lower momentum (dashed lines). This is a direct reflection of the ordinary concept of density accumulation in the bond region. However, at $R = 1$ a.u., a small but nonnegligible density increase appears for $p > 1.4$ a.u. This expansion of momentum density seems responsible for positive ΔE at this separation, since the expansion may cancel the contraction in the range of $0 < p < 1.4$ a.u. due to the weighting factor (kinetic operator) $p^2/2$.

For $R \geq 4$ a.u., $\Delta\tilde{I}$ shows contraction corresponding to the attraction in F. At $R = R_e$, the guiding principle [1] suggests that $\Delta\tilde{I}$ must show a critical feature of contraction and expansion since F vanishes at this point. However, the character of contraction is dominant even at $R_e = 2$ a.u. and the critical nature of the reoganization $\Delta\tilde{I}$ is not clear. (Finer analysis shows a small expansion for $p > 2.1$ a.u., which just balances the contraction.) For $R = 1$ a.u., expansion is observed for $p > 1.1$ a.u. and this is the origin of repulsion at $R < R_e$.

The atom-bond partitioning in Fig. 2 shows a predominant contribution of the atomic part in both ΔT and ΔE. Regional atom–bond analysis in coordinate space [11] also gave the same trend. This seems to be a result of density flow from the atomic to the bond part. (Integration of the partitioned densities assigns the

electronic charges of $1/(1+S)$ and $S/(1+S)$ to the atomic and bond parts, respectively.) The decrease in the atomic density may cause a decrease of the kinetic pressure in this portion, which contributes to lower the kinetic energy and then the total energy. (On the relation between the kinetic and total energies, see Ref. 1.) However, for $R = R_e$, Fig. 2 shows that the atomic part is still decreasing with decreasing R, and it is the increase in the bond part that causes the ΔE curve to turn up for $R < R_e$. Thus the atomic part is dominant in the initiation and acceleration of bond formation while the bond part is important in the termination of the process or the determination of R_e as well as the atomic part.

In this relation, it may be interesting to note that Pearson [19] recently reported a possibility of covalent bonding from the classical density. He suggested that the major part of the stabilization accompanied with bond formation can be explained by the simple superposition of atomic densities. He also showed that the dominant origin of this stabilization is the lowering of the kinetic energy.

Also plotted in Fig. 2 is the directional partitioning of ΔT and ΔE into the parallel ($\|$) and perpendicular ($\perp$) components. Of the two components, the $\|$ part is shown to be dominant and to contribute to the stabilization of the system until very small R. As shown in Fig. 4a, this is a result of contraction of momentum density in this direction, which corresponds to the coordinate-space concept of decrease in the kinetic pressure due to the extension of the space of electronic motion from

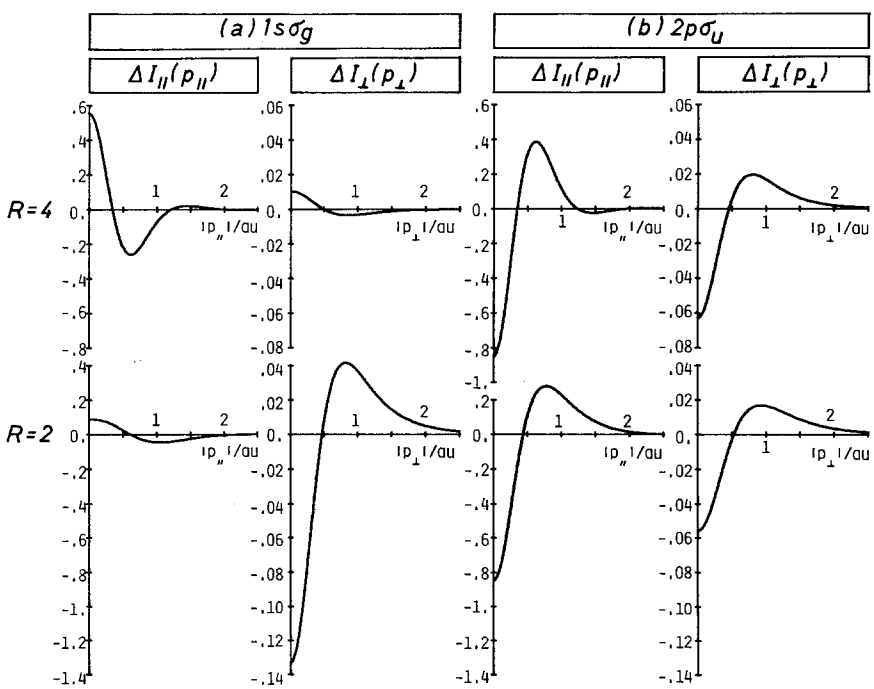

Fig. 4. Differences in the directional momentum densities. All values in atomic units. (a) $1s\sigma_g$ state. (b) $2p\sigma_u$ state

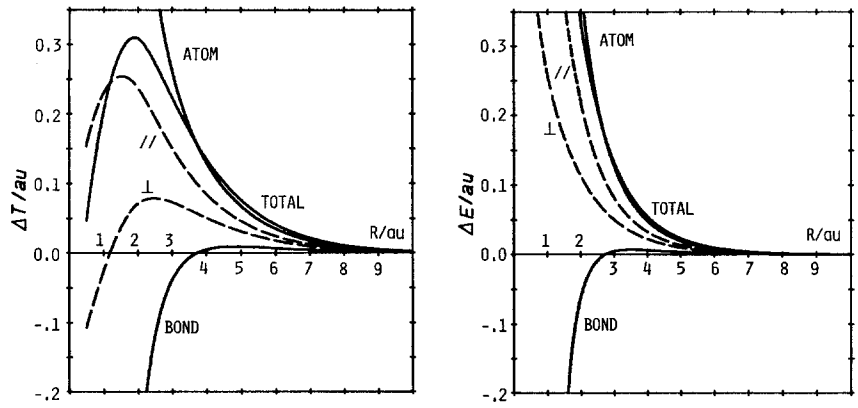

Fig. 5. $2p\sigma_u$ state. See the captions of Fig. 2

atoms to molecule. The significance of this component is in agreement with the results of Feinberg and Ruedenberg [11] and of Hoare and Linnett [20] that the parallel component of the kinetic energy is most critical for bonding. The contribution of the $\perp$ component is initially stabilizing but changes into destabilization for $R < 2.1$ a.u.. Corresponding contraction and expansion are seen in the $\Delta I_\perp$ plots (Fig. 4a). The increase in the orbital exponent seems mainly responsible for the expansion. Similar to the role of the bond part in the atom–bond partitioning, the $\perp$ component is an essential origin of the termination of reaction in the directional partitioning. This point recalls us a defect of the one-dimensional box model of diatomic molecules which contains only the $\parallel$ component. The model gives the energy $E_n = n^2\pi^2/2R^2$ (n denotes the quantum number and R the box length) and does not show any minimum in energy against R.

4.2. $2p\sigma_u$ State

In Fig. 5, the results for ΔT and ΔE obtained from the momentum density are plotted together with their atom–bond and parallel-perpendicular decompositions.

All the density origins ΔI, $\Delta \bar{I}$, and $\Delta \tilde{I}$ given in Fig. 6 show the increasing expansions with decreasing R, which are responsible for the monotonous increase in ΔT, ΔE, and F. These expansion results from the migration of the low-momentum bond density to the high-momentum atomic density (see the dashed lines for $R = 2$ a.u. in Fig. 6). The amounts of the atomic and bond charges are respectively $1/(1-S)$ and $-S/(1-S)$ in this state.

As a result, the atomic part is the predominant origin of the destabilization (Fig. 5). The bond component is slightly destabilizing for $R > 3$ a.u. but becomes stabilizing for smaller separations. The latter contribution of the bond part may be attributed mainly to the decrease in bond charge which would be effective to lower the kinetic pressure. The amount of electrons in the partitioned densities

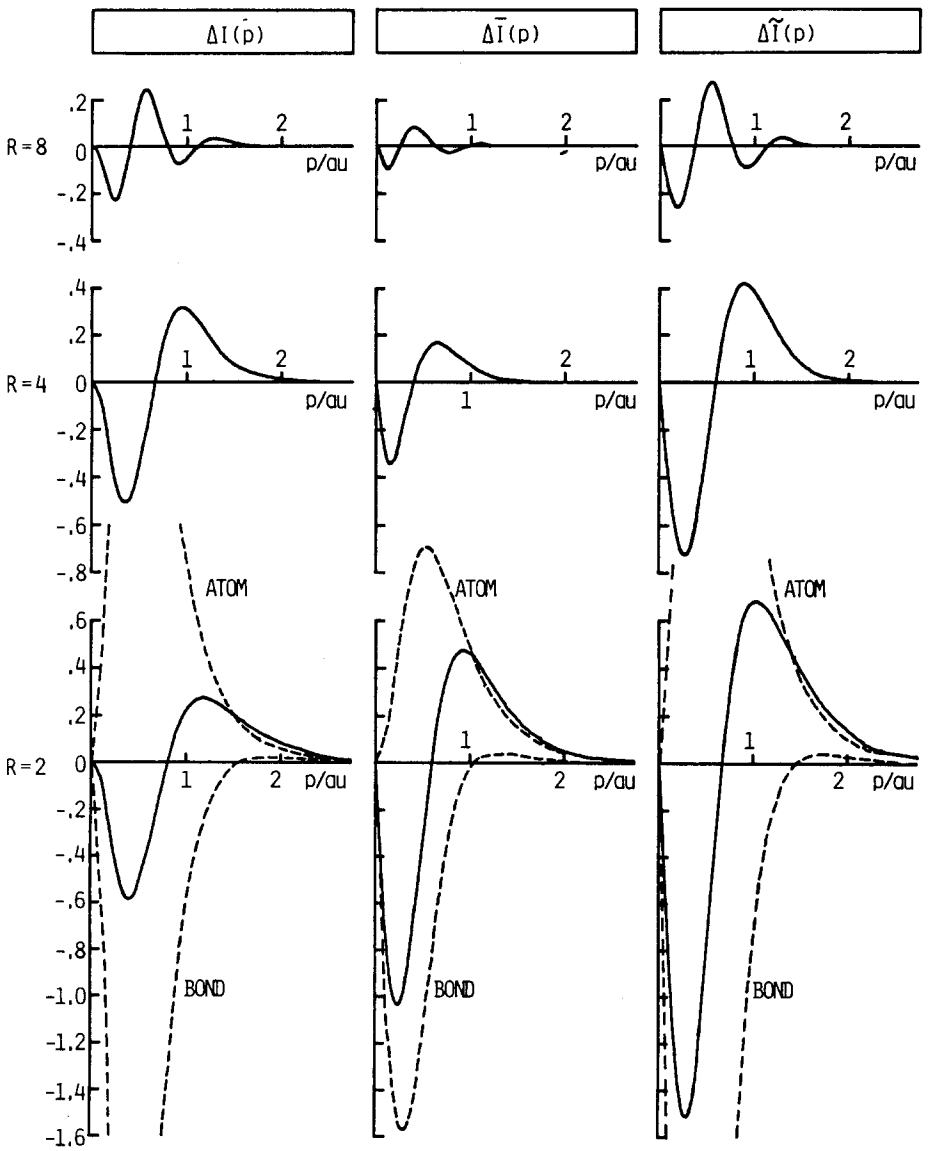

Fig. 6. $2p\sigma_u$ state. See the captions of Fig. 3

seems to be an important factor as in the ground $1s\sigma_g$ state. It is surprising for us that the amount of electronic charge plays a different role in the two spaces; e.g. a decrease of the bond density in the coordinate space contributes to destabilize the system, whereas a decrease of the bond density in the momentum space contributes to stabilize the system.

In the directional partitioning, both the $\parallel$ and $\perp$ components cooperatively work to destabilize the system. The corresponding expansions are found in the density differences $\Delta I_{\parallel}$ and $\Delta I_{\perp}$ depicted in Fig. 4b. The presence of a nodal plane $p_z = 0$ works to transfer momentum density from the low momentum region around the origin to the high momentum region (see Fig. 1). This induces the expansion in both the $\parallel$ and $\perp$ directions.

The results discussed above for the $1s\sigma_g$ and $2p\sigma_u$ states suggest that the atomic and parallel parts are of primary importance for the initial and intermediate stages. They seem to characterize the process of interaction in momentum space. However, the bond and perpendicular components as well play a significant role in the final stage. The equilibrium distance results from the balance of the two opposing contributions of the atomic and bond parts, or of the parallel and perpendicular parts.

Summary

The recently proposed method of momentum density has been applied to the simple but actual system of H_2^+ using the Finkelstein–Horowitz wave function. The results for the bonding $1s\sigma_g$ and antibonding $2p\sigma_u$ states show the validity of the guiding rule of contraction and expansion for the behaviour of momentum density. Stabilization (attraction) and destabilization (repulsion) of the system have been interpreted based on the reorganization of the momentum density. Two partitionings of the stabilization energy have been carried out for the process of interaction. In the atom–bond partitioning, the atomic part has been shown to be important as the origin of bonding. A decrease in atomic density rather than an increase in bond density is essential for the stabilization. In the directional partitioning, the parallel component has been predominant in accordance with the previous discussion in the coordinate space.

Acknowledgment. Part of this study has been supported by a Grant-in-Aid for Scientific Research from the Ministry of Education of Japan.

References

1. Koga, T.: Theoret. Chim. Acta (Berl.), **58**, 173 (1981)
2. Hurley, A. C.: Proc. Roy. Soc. London, **A226**, 170 (1954)
3. Nalewajski, R. F.: Chem. Phys. Letters **54**, 502 (1978); Nalewajski, R. F.: Intern. J. Quantum Chem. **S12**, 87 (1978)
4. Cooper, M.: Adv. Phys. **20**, 453 (1971); Epstein, I. R.: Acc. Chem. Res. **6**, 145 (1973); Epstein, I. R., in: International review of science. Physical chemistry. Ser. 2. Vol. 1. Theoretical chemistry,

pp. 107–161. Buckingham, A. D., Coulson, C. A., ed. London: Butterworths 1975; Williams, B. G. ed.: Compton scattering, New York: McGraw-Hill 1977; Kaijser, P., Smith, Jr., V. H.: Adv. Quantum Chem. **10**, 37 (1977).
5. Bates, D. R., Ledsham, K., Stewart, A. L.: Phil. Trans. Roy. Soc. London **A246**, 215 (1954); Bates, D. R., Reid, R. H. G.: Adv. At. Mol. Phys. **4**, 13 (1968); Teller, E., Sahlin, H. L., in: Physical chemistry. An advanced treatise, Vol. 5. Valency, pp. 35–124, Eyring, H., ed. New York: Academic Press 1970
6. Glaser, F. M., Lassettre, E. N.: J. Chem. Phys. **44**, 3787 (1966)
7. Guillemin, V., Zener, C.: Proc. Natl. Acad. Sci. U. S. **15**, 314 (1929); Kim, S., Chang, T. Y., Hirschfelder, J. O.: J. Chem. Phys. **43**, 1092 (1965)
8. James, H. M.: J. Chem. Phys. **3**, 9 (1935)
9. Duncanson, W. E.: Proc. Camb. Phil. Soc. **37**, 397 (1941)
10. Finkelstein, B. N., Horowitz, G. E.: Z. Phys. **48**, 118 (1928); Coulson, C. A.: Trans. Faraday Soc. **33**, 1479 (1937); Dalgarno, A., Poots, G.: Proc. Phys. Soc. **A67**, 343 (1953)
11. Feinberg, M. J., Ruedenberg, K., Mehler, E. L.: Adv. Quantum Chem. **5**, 27 (1970); Feinberg, M. J., Ruedenberg, K.: J. Chem. Phys. **54**, 1495 (1971); Ruedenberg, K., in: Localization and delocalization in quantum chemistry. Vol. 1. Atoms and molecules in the ground state, pp. 223–245; Chalvet, O., Daudel, R., Diner, S., Malrieu, J. M. Ed. Dordrecht-Holland: D. Reidel 1975
12. Steiner, E.: The determination and interpretation of molecular wave functions. London: Cambridge U.P. 1976; Mulliken, R. S., Ermler, W.: Diatomic molecules. New York: Academic Press 1977; Hurley, A. C.: Introduction to the electron theory of small molecules. New York: Academic Press 1976
13. Löwdin, P.-O.: J. Mol. Spectrosc. **3**, 46 (1969); Löwdin, P.-O.: Adv. Chem. Phys. **2**, 207 (1959)
14. Coulson, C. A.: Proc. Camb. Phil. Soc. **37**, 55 (1941)
15. Goodisman, J.: Contemporary quantum chemistrty, pp. 36–38. New York: Plenum Press 1977; Goodisman, J.: Diatomic interaction potential theory. Vol. 2. Applications. p. 352. New York: Academic Press 1973
16. Arnold, J. R.: J. Chem. Phys. **22**, 757 (1954); **24**, 181 (1956)
17. Denaro, A. R.: A foundation for quantum chemistry. London: Butterworths 1975; Morrison, A. M., Estle, T. L., Lane, N. F.: Quantum states of atoms, molecules, and solids. New Jersey: Prentice-Hall 1976
18. Abramowitz, M., Stegun, I. A., ed.: Handbook of mathematical functions. New York: Dover 1970; Gradshteyn, I. S., Ryzhik, I. M.: Table of integrals, series, and products. New York: Academic Press 1965
19. Pearson, R. G.: Theoret. Chim. Acta (Berl.) **52**, 253 (1979); **54**, 340 (1980); Pearson, R. G., Palke, W. E.: Proc. Natl. Acad. Sci. U. S. **77**, 1725 (1980)
20. Hoare, M. F., Linnett, J. W.: Trans. Faraday Soc. **46**, 885 (1950)

Received November 25, 1980/February 3, 1981